Rothamsted Repository Download

A - Papers appearing in refereed journals

Eastmond, P. J., Van-Erp, H., Bryant, F. M., Martin-Moreno, J. and Michaelson, L. V. 2021. Production of the infant formula ingredient 1,3-olein-2-palmitin in Arabidopsis thaliana seeds. *Metabolic Engineering.* 67, pp. 67-74. https://doi.org/10.1016/j.ymben.2021.05.009

The publisher's version can be accessed at:

- https://doi.org/10.1016/j.ymben.2021.05.009

The output can be accessed at:

https://repository.rothamsted.ac.uk/item/984wz/production-of-the-infant-formula-ingredient-1-3-olein-2-palmitin-in-arabidopsis-thaliana-seeds.

© 4 June 2021, Please contact library@rothamsted.ac.uk for copyright queries.

1 **Title of article:**

2

3 Production of the infant formula ingredient 1,3-olein-2-palmitin in *Arabidopsis thaliana* seeds

4

5

6 **Authors' names:**

7

8 Harrie van Erp, Fiona M Bryant, Jose Martin-Moreno, Louise V. Michaelson, Peter J Eastmond[1]

9

10 **Addresses:**

11

12 Plant Science Department, Rothamsted Research, Harpenden, Hertfordshire, AL5 2JQ, UK

13

14 **Correspondence:**

15

16 [1]Peter J. Eastmond**,** Rothamsted Research**,** Harpenden**,** Hertfordshire AL5 2JQ, UK; E-mail:
17 peter.eastmond@rothamsted.ac.uk**;** Tel: +44 (0) 1582 763133**;** Fax: +44 (0) 1582 763010

18

22
23

ABSTRACT

In human milk fat, palmitic acid (16:0) is esterified to the middle (sn-2 or β) position on the glycerol backbone and oleic acid (18:1) predominantly to the outer positions, giving the triacylglycerol (TG) a distinctive stereoisomeric structure that is believed to assist nutrient absorption in the infant gut. However, the fat used in most infant formulas is derived from plants, which preferentially esterify 16:0 to the outer positions. We have previously showed that the metabolism of the model oilseed *Arabidopsis thaliana* can be engineered to incorporate 16:0 into the middle position of TG. However, the fatty acyl composition of Arabidopsis seed TG does not mimic human milk, which is rich in both 16:0 and 18:1 and is defined by the high abundance of the TG molecular species 1,3-olein-2-palmitin (OPO). Here we have constructed an Arabidopsis *fatty acid biosynthesis 1-1 fatty acid desaturase 2 fatty acid elongase 1* mutant with around 20% 16:0 and 70% 18:1 in its seeds and we have engineered it to esterify more than 80% of the 16:0 to the middle position of TG, using heterologous expression of the human lysophosphatidic acid acyltransferase isoform AGPAT1, combined with suppression of LYSOPHOSPHATIDIC ACID ACYLTRANSFERASE 2 and PHOSPHATIDYLCHOLINE:DIACYLGLYCEROL CHOLINEPHOSPHOTRANSFERASE. Our data show that oilseeds can be engineered to produce TG that is rich in OPO, which is a structured fat ingredient used in infant formulas.

1. Introduction

Human milk is considered the optimal source of nutrition for infants and it is their main food during the first 4–6 months of life (Innis 2011; Wei et al., 2019). The lipid fraction provides approximately half the infant's calories and mainly consists of triacylglycerols (TG), which account for about 98% of total lipids (Wei et al., 2019). Palmitic acid (16:0) is the most abundant saturated fatty acid (FA) in human milk, providing about 20–25% of the total milk FAs (Wei et al., 2019). In human milk, over 70% of this 16:0 is esterified to the middle (sn-2 or β) position on the glycerol backbone of TG, while unsaturated FA, such as oleic acid (18:1), occupy the outer (sn-1/3 or α) positions (Breckenridge et al., 1969; Giuffrida et al., 2018). This allow greater efficiency of 16:0 absorption and utilization in infants when compared to infants fed with TG containing 16:0 preferentially esterified to the sn-1/3 positions (Innis 2011; Béghin et al., 2018).

56 This is because during digestion, lipases release FAs preferentially from the sn-1/3 positions of

57 TG to produce free FA and 2-monoacylglycerols (Innis 2011; Béghin et al., 2018). 16:0

58 esterified to the sn-2 position of monoacyglycerol is easily absorbed while free 16:0 tends to

59 form insoluble calcium soaps (Innis 2011; Béghin et al., 2018).

60 In infant formulas the lipid phase is usually provided by a mixture of vegetable fats and

61 oils, blended to mimic the FA composition of human milk (Wei et al., 2019). However, plants

62 virtually always exclude 16:0 from the sn-2 position of their TG (Brockerhoff and Yurkowsk,

63 1966; Christie et al., 1991) and therefore vegetable fats cannot mimic the regiospecific

64 distribution of 16:0 that is found in human milk. To address this problem several companies have

65 developed human milk fat substitutes (HMFS) that are produced by enzyme-catalyzed acidolysis

66 (or alcoholysis and esterification) of fractionated vegetable fats and free FA using sn-1/3-

67 regioselective lipases (Wei et al., 2019). These HMFS contain TG with substantial levels of 16:0

68 enrichment at the sn-2 position and are widely use as ingredients in infant formulas (Wei et al.,

69 2019). However, they are relatively costly to make, and it remains technically challenging to

70 manufacture a true mimetic that allows over 70% of 16:0 to be esterified to the sn-2 position in

71 the final lipid phase (Ferreira-Dias and Tecelão, 2014).

72 For this reason, we decided to investigate whether plant lipid metabolism can be

73 engineered to directly produce TG with 16:0 enrichment at the sn-2 position (van Erp et al.,

74 2019). TG is formed by a cytosolic glycerolipid biosynthetic pathway on the endoplasmic

75 reticulum (ER) and the enzyme responsible for acylation of the sn-2 position is lysophosphatidic

76 acid acyltransferase (LPAT) (Fig. 1) (Ohlrogge and Browse, 1995). ER-localized LPAT isoforms

77 discriminate against a 16:0-Coenzyme A (CoA) substrate (Kim et al., 2005). By contrast,

78 chloroplast-localized LPAT isoforms are highly selective for 16:0-acyl carrier protein (ACP) and

79 will also accept 16:0-CoA (Joyard and Douce, 1977; Frentzen et al., 1983). We therefore

80 modified a chloroplast LPAT by removing its targeting signal so that it localizes to the ER

81 (ΔCTS-LPAT1 or mLPAT1) and expressed it in the model oilseed *Arabidopsis thaliana*, where

82 it esterified more than 30% of 16:0 at the sn-2 position of TG (van Erp et al., 2019). By

83 disrupting LPAT2 we were then able to increase the percentage of 16:0 at sn-2 to around 50%

84 (van Erp et al., 2019). LPAT2 is the main ER-localized LPAT isoform expressed in Arabidopsis

85 seeds (Kim et al., 2005) and therefore it likely competes with mLPAT1 (Fig. 1) (van Erp et al.,

86 2015). Finally, we achieved a further increase in the percentage of 16:0 at sn-2 of TG to around

87 70% by disrupting phosphatidylcholine:diacylglycerol cholinephosphotransferase (PDCT) (Lu et

88 al., 2009). More than 90% of the glyceryl groups in Arabidopsis seed TG are derived from

89 phosphatidylcholine (PC) owing to rapid diacylglycerol (DG) – PC interconversion, catalyzed

90 mainly by the head group exchange enzyme PDCT (Bates et al., 2012). Although LPAT initially

91 acylates glycerolipids at sn-2, once these acyl groups are in PC they can be modified by ER-

92 localized acyl-lipid desaturases such as FATTY ACID DESATURASE 2 (FAD2) (Miquel and

93 Browse, 1992; Okuley et al., 1994) and/or be replaced by a deacylation-reacylation (acyl editing)

94 cycle (Stymne and Stobart, 1984; Wang et al., 2012; Bates et al., 2012). Disruption of PDCT

95 therefore forces a more direct flux of newly made DG into TG, helping to bypass PC (Fig. 1)

96 (Bates et al., 2012).

97
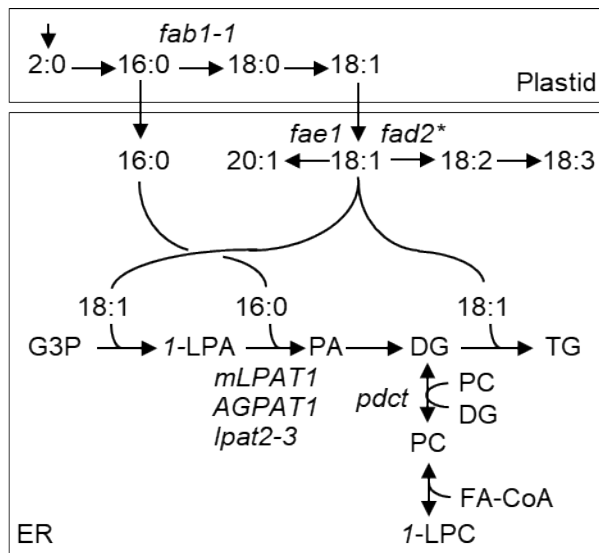
98

99 **Fig. 1. A simplified diagram illustrating the strategy used in this study to produce OPO in**

100 **Arabidopsis seeds.** A combination of the hypomorphic *fab1-1* and null *fae1* and *fad2* mutant

101 alleles was used to produce high levels of 16:0 and 18:1 in seeds. Expression of an ER-localised

102 LPAT with 16:0-CoA preference combined with a hypomorphic *lpat2-3* and null *pdct* mutant

103 allele was then used to enable 16:0 to be preferentially esterified to the sn-2 position of *1*-LPA

104 and the products channelled into TG. 16:0, palmitic acid; 18:1, oleic acid; CoA, Coenzyme A;

105 G3P, glycerol-3-phosphate; *1*-LPA, sn-1 lysophosphatidic acid; PA, phosphatidic acid, DG,

106 diacylglycerol, TG, triacylglycerol; PC, phosphatidylcholine; *1*-LPC, sn-1

107 lysophosphatidylcholine; FA, fatty acid. * denotes that FAD2 uses an acyl group esterified to PC

108 as a substrate.

4

109

Although our work has showed that plant lipid metabolism can be engineered to esterify 16:0 to the sn-2 position in TG (van Erp et al., 2019), the total FA composition of Arabidopsis seeds does not resemble human milk and the TG we produced would not be appropriate for use as an infant formula ingredient. 16:0 is around 3-fold less abundant in Arabidopsis seeds and they contain a high proportion of polyunsaturated and very-long-chain FA species that are essentially absent from human milk (Giuffrida et al., 2018). The most abundant FA in human milk is 18:1 and, because of the unusual regiospecific distribution of the next most abundant FA 16:0, the major molecular species of TG is 1,3-olein-2-palmitin (OPO), usually accounting for more than 14% of the total (Giuffrida et al., 2018). Infant formula manufacturers would benefit most from a pure source of OPO, because this can easily be blended with vegetable fats and oils to produce a final lipid phase that mimics human milk. The aim of this study was to investigate whether an oilseed can be engineered to produce OPO, by combining 16:0 enrichment at the sn-2 position in TG with a total FA composition rich in the appropriate ratio of 16:0 and 18:1.

2. Materials and methods

2.1. Plant material and growth conditions

The *Arabidopsis thaliana* Colombia-0 mutants *fab1-1*, *fae1*, *fad2*, *pdct* and *lpat2-3* have been described previously (Wu et al., 1994; Smith et al., 2003; Lu et al., 2009; van Erp et al., 2019). The *fab1-1*, *fae1*, *fad2* and *pdct* mutants contain single nucleotide polymorphisms induced by ethyl methanesulfonate treatment that cause non-synonymous substitutions, whereas *lpat2-3* carries a T-DNA insertion in the gene promoter that reduces *LPAT2* transcript abundance. The *fab1-1* and *lpat2-3* mutants are hypomorphs and we used these alleles because amorphic mutations are lethal (Pidkowich et al., 2007; Kim et al., 2005). For experiments performed on media, about 50 seeds from individual plants were surface sterilized, plated on agar plates containing one-half strength Murashige and Skoog salts (Sigma-Aldrich) pH 5.7 and imbibed in the dark for 4 d at 4°C. The plates were then placed in a growth chamber set to 16-h light (photosynthetic photon flux density = 150 μmol m^{-2} s^{-1}) / 8-h dark cycle at a constant temperature of 20°C. Germination (radicle emergence) and cotyledon expansion was scored

140 visually under a dissecting stereomicroscope as described previously (van Erp et al., 2019).

141 Individual seedlings were also transplanted to 7 cm^2 pots containing Levington F2 compost and

142 grown in a chamber set to a 16-h light (22 °C) / 8-h dark (16 °C) cycle, with a photosynthetic

143 photon flux density of 250 μmol m^{-2} s^{-1}. The plants were bagged individually at the onset of

144 flowering and the seeds were harvested at maturity.

145

146 *2.2. Genotyping*

147

148 Genomic DNA was isolated from leaves using the DNeasy Plant Mini Kit (Qiagen).

149 Homozygous *lpat2-3* T-DNA insertional mutants were identified by PCR using Promega PCR

150 Master Mix (Promega) and combinations of the gene specific and T-DNA left border primers

151 pairs, as described previously (van Erp et al., 2019). Homozygous *fab1-1*, *fad2*, *fae1* and *pdct*

152 mutants were identified by sequencing PCR products amplified with primer pair spanning the

153 sites of the point mutations (Wu et al., 1994; Smith et al., 2003; Lu et al., 2009). The presence of

154 *ProGLY:mLPAT1* and *ProGLY:AGPAT1* T-DNAs was determined by PCR using a primer pair

155 spanning *ProGLY* and *mLPAT1* or *AGPAT1* (van Erp et al., 2019).

156

157 *2.3. Lipid analysis*

158

159 Total lipids were extracted from material and TG was purified as described previously (Kelly et

160 al., 2013). TG regiochemical analysis was performed by lipase digestion following the method

161 described previously (van Erp et al., 2011), except that *2*-monoacylglycerols were separated by

162 thin layer chromatography (Silica gel 60, 20 x 20 cm; Sigma-Aldrich/Merck) using

163 hexane:diethylether:acetic acid (35:70:1.5, v/v/v) (Bates et al., 2011). Fatty acyl groups present

164 in whole seeds and purified lipid fractions are expressed at mol% and were trans-methylated and

165 quantified by gas chromatography (GC) coupled to flame ionization detection, as described

166 previously (van Erp et al., 2019), using a 7890A GC system fitted with DB-23 columns (30 m x

167 0.25 mm i.d. x 0.25 μm) (Agilent Technologies). TG molecular species composition was

168 analysed by high resolution / accurate mass (HR/AM) lipidomics using a Vanquish - Q Exactive

169 Plus UPLC-MS/MS system (Thermo Fisher Scientific), using a workflow that has been

170 described previously (West et al., 2020). Seed oil and moisture contents of whole seeds were

171 measured by low-resolution time domain NMR spectroscopy using a Minispec MQ20 device

172 (Bruker) fitted with a robotic sample-handling system (Rohasys) as described previously (van

173 Erp et al., 2014) and the percentage oil content was normalised to 9% moisture.

174

175 *2.4. Cloning and transformation*

176

177 *H. sapiens* AGPAT1 (GenBank: NP_001358367) was codon optimised for expression in

178 Arabidopsis, synthesised by Genscript and supplied in pUC57. AGPAT1 was then amplified by

179 PCR   with   KOD   DNA   polymerase   (Merck)   using   primer   pair   5'-

180 CACCATGGATTTATGGCCTGGTGC-3' & 5'-TCATCCTCCTCCACCTGG-3'. The resulting

181 PCR product was purified with the QIAquick Gel Extraction Kit (Qiagen). The PCR product was

182 cloned in the pENTR/D-TOPO vector (Thermo Fisher Scientific), sequenced and recombined

183 into pK7WGR2 (Vlaams Institute for Biotechnology) using the Gateway LR Clonase II Enzyme

184 mix (Thermo Fisher Scientific). AGPAT was cloned in the pBinGlyRed3 vector in between the

185 soybean glycinin-1 (GLY) promoter and terminator for seed specific expression (Zhang et al.,

186 2013). AGPAT1 was PCR-amplified from the pENTR-D-TOPO vector using KOD DNA

187 polymerase   and   primer   pair   5'-CGGAATTCATGGATTTATGGCCTGGTGC-3'   &   5'-

188 GCTCTAGATCATCCTCCTCCACCTGG-3'. The PCR product was gel purified and digested

189 with EcoRI and XbaI. The pBinGlyRed3 vector was also digested with EcoRI and XbaI, alkaline

190 phosphatase treated (Promega), gel purified and AGPAT1 was ligated into the vector using T4

191 DNA ligase (NEB). Heat shock was used to transform the pK7WGR2 and pBinGlyRed3 vectors

192 into *Agrobacterium tumefaciens* strain GV3101. Arabidopsis transformation was carried out

193 using the floral-dip method (Clough and Bent, 1998). T1 seeds expressing the selectable marker

194 were identified under a Leica M205 FA microscope using the DsRed filter.

195

196 *2.5. Transient expression in N. benthamiana and imaging*

197

198 Transient expression in *N. benthamiana* leaves was carried out as described by Wood et al.,

199 (2009) using *A. tumefaciens* cultures transformed with vectors harbouring *Pro35S:RFP-

200 AGPAT1*, *Pro35S:m-GFP5-ER* or *Pro35S:p19*. Cultures were hand-infiltrated into leaves and the

201 inoculated plants were left for 48 h. *N. benthamiana* leaves were then mounted in water on a

202 Zeiss LSM 780 laser scanning confocal microscope under an Apochromat 63x/1.20 W Korr M27
203 objective. The GFP signal was excited using the 488 nm laser and the emitted fluorescence was
204 collected at 473-551 nm, whereas RFP was excited using the 561 nm laser and the emitted
205 fluorescence collected at 570- 640 nm.

206

207 *2.6. Statistical analyses*

208

209 All experiments were carried out using more than three biological replicates and the data are
210 presented as the mean values ± standard error of the mean (SE). For statistical analysis we either
211 used one-way analysis of variance (ANOVA) with post-hoc Tukey HSD (Honestly Significant
212 Difference) tests, or two-tailed Student's t-tests.

213

214 *2.7. Accession numbers*

215

216 Sequence data from this article can be found in the GenBank/EMBL data libraries under
217 accession numbers: NP_001358367 (AGPAT1), AF111161 (LPAT1), At1g74960 (FAB1),
218 At3g12120 (FAD2), At4g34520 (FAE1), At3g57650 (LPAT2), At3g15820 (PDCT).

219

220 **3. Results**

221

222 *3.1. Seed of fab1-1 fae1 fad2 are high in 16:0 and 18:1 (HPHO)*

223

224 To obtain Arabidopsis seeds with 16:0 content equivalent to human milk, the level must be
225 increased around 3-fold to 20-25%. One approach to achieve this is to reduce fatty acid synthase
226 catalysed 16:0 elongation by disrupting the β-ketoacyl-ACP synthase II gene *FATTY ACID*
227 *BIOSYNTHESIS 1* (*FAB1*) (Fig. 1) (Wu et al., 1994; Carlsson et al., 2002). *FAB1* is an essential
228 gene in Arabidopsis (Pidkowich et al., 2007), but a single hypomorphic *fab1-1* allele has been
229 characterised that contains around 17% 16:0 in its seeds (Wu et al., 1994; Carlsson et al., 2002).
230 In *fab1-1*, 16:0 can then be increased to about 24% by disrupting FATTY ACID ELONGASE 1
231 (FAE1) (James and Dooner, 1991), which is required for very-long-chain fatty acid synthesis
232 (Fig. 1) (James et al., 1995; Millar and Kunst, 1997). However, *fab1-1 fae1* seeds still contain a

8

233   high proportion of polyunsaturated fatty acids (James and Dooner, 1991), produced by the acyl-

234   lipid desaturase FAD2 (Fig. 1) (Miquel and Browse, 1992; Okuley et al., 1994). To create a

235   background high both 16:0 and 18:1 (HPHO) we therefore constructed a *fab1-1 fae1 fad2* triple

236   mutant by crossing. Analysis of homozygous *fab1-1 fae1 fad2* seeds showed that the FA

237   composition of the TG is high in 16:0 and 18:1, which account for around 20 and 70% for total

238   FA, respectively (Fig. 2). Other FA species that are normally abundant in wild type Arabidopsis

239   Col-0 seed TG, such as linoleic acid (18:2), linolenic acid (18:3) and eicosenoic acid (20:1), each

240   account for less than 3% (Fig. 2). Comparison with the double mutants showed that 16:0 content

241   in *fab1-1 fae1* is reduced significantly ($P > 0.05$) in the *fad2* background (Fig. 2). Nevertheless,

242   the HPHO composition of *fab1-1 fae1 fad2* suggests that this genetic background is appropriate

243   to test whether OPO can be produced in seeds.
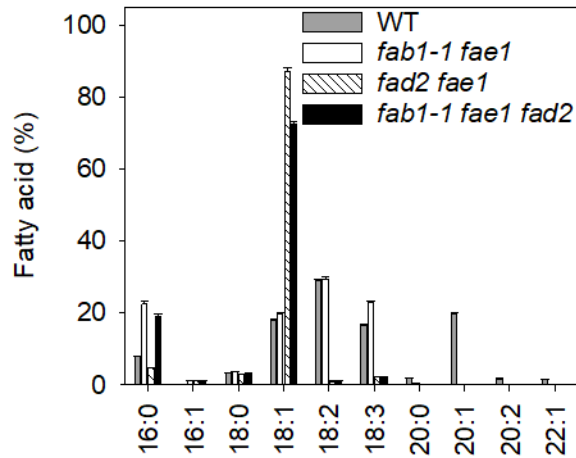
Fig. 2. FA composition of TG from HPHO seeds. Total FA composition of TG isolated from WT, *fab1-1 fae1, fad2 fae1* and *fab1-1 fae1 fad2* seeds. Values are the mean ± SE of measurements on seeds from three plants of each genotype.

3.2. mLPAT1 expression in HPHO seed drives 16:0 incorporation into the sn-2 position of TG

We have previously shown that expression of an ER-retargeted version of the chloroplast LPAT (ΔCTS-LPAT1 or mLPAT1) in WT Arabidopsis seeds, under the soybean glycinin-1 promoter (*ProGLY*), leads to a substantial increase in esterification of 16:0 to the sn-2 position in TG (van Erp et al., 2019). To determine what effect mLPAT1 expression has in a HPHO background, we constructed a *ProGLY:mLPAT1 fab1-1 fae1 fad2* line by crossing. When we purified TG from the seeds and performed positional analysis (van Erp et al., 2019), we found that the percentage of 16:0 at the sn-2 position (versus sn-1+3), had increased from about 3% in the *fab1-1 fad2 fae1* background to around 24% in *ProGLY:mLPAT1 fab1-1 fad2 fae1* (Fig. 3A). The total FA composition of *fab1-1 fad2 fae1* seeds was not altered greatly by mLPAT1 expression, except that there was a significant ($P > 0.05$) increase in 16:0 abundance, from about 19 to 22% (Fig. 3B). We previously observed an increase in total 16:0 content when we expressed mLPAT1 in WT seeds (van Erp et al., 2019; Fig. 3B). Our data show that mLPAT1 expression in HPHO seeds allows incorporation of 16:0 into the sn-2 position of TG. However, the level of enrichment is significantly lower ($P > 0.05$) than in WT seeds containing *ProGLY:mLPAT1* (Fig. 3A).

267
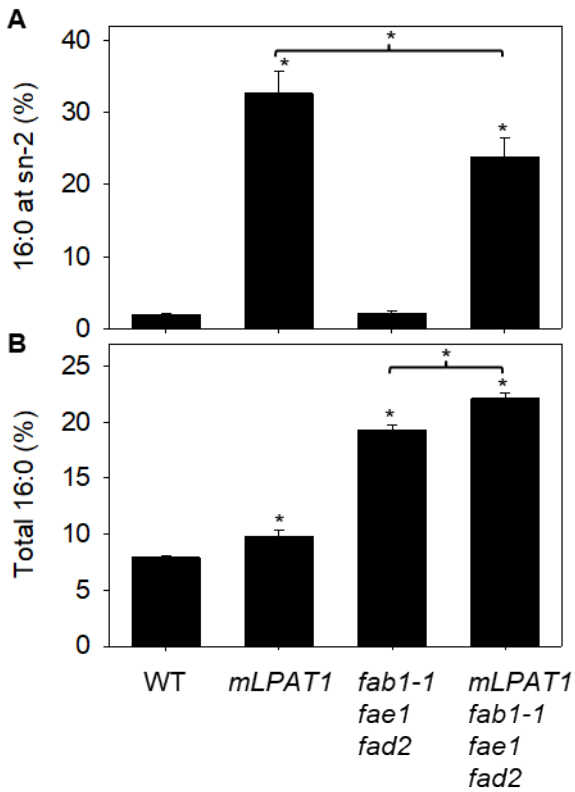
Fig. 3. 16:0 in TG from WT and HPHO seeds expressing *mLPAT1*. Percentage of 16:0 esterified to the sn-2 position (A) and 16:0 as a percentage of total FA content (B) measured in TG isolated from WT, *ProGLY:mLPAT1*, *fab1-1 fad2 fae1* and *ProGLY:mLPAT1 fab1-1 fad2 fae1* seeds. Values are the mean ± SE of measurements on seeds from three plants of each genotype. * denote values significantly (P < 0.05) different either from WT or, where marked in parenthesis, from one another (ANOVA + Tukey HSD test).

3.3. AGPAT1 expression drives stronger 16:0 incorporation into the sn-2 position of TG

To investigate whether other ER-localised LPATs might enable Arabidopsis to incorporate more 16:0 into the sn-2 position of TG than mLPAT1, we decided to test *Homo sapiens* AGPAT1 (Agarwal et al., 2011). Human milk fat globules are secreted by lactocytes in the mammary gland epithelium (Witkowska-Zimny and Kaminska-El-Hassan, 2017). It is not known precisely which LPAT is responsible for human milk fat biosynthesis. However, *AGPAT1* is expressed in mammary epithelial cells (Lamay et al., 2013) and *in vitro* assays suggest that AGPAT1 can use 16:0-CoA as a substrate (Agarwal et al., 2011). Using transient expression in *Nicotiana*

11

283　*benthamiana* leaves, we confirmed that AGPAT1 can localise to the ER in plant cells when it is

284　expressed as a red fluorescent protein (RFP)-AGPAT1 fusion protein under the cauliflower

285　mosaic virus 35S promoter (Fig. 4A). Next we transformed WT Arabidopsis plants with a

286　*ProGLY:AGPAT1* construct in order to drive strong seed-specific expression of the transgene

287　(van Erp et al., 2019). We selected 44 primary transformants using the DsRed fluorescent marker

288　system (Zhang et al., 2013) and screened the T2 seeds for an enrichment of tripalmitin

289　(16:0_16:0_16:0), which we previously found is a marker for increased 16:0 esterification at the

290　sn-2 position in TG (van Erp et al., 2019). The transgenic lines exhibited up to a 20-fold increase

291　in tripalmitin (Supplementary Table 1) and we selected two single copy lines (L35 & L40) for

292　further analysis. When we purified TG from the homozygous T3 seed batches and carried out

293　positional analysis, we found that the percentage of 16:0 at the sn-2 position was about 66% for

294　L40 and 74% for L35 (Fig. 4B). To determine what effect AGPAT1 expression has in the HPHO

295　background we constructed a *ProGLY:AGPAT1 fab1-1 fae1 fad2* line by crossing L35. When we

296　purified TG from these seeds and performed positional analysis, we found that the percentage of

297　16:0 at the sn-2 position was around 54% (Fig. 4B). The total 16:0 content of *ProGLY:AGPAT1*

298　*fab1-1 fae1 fad2* seeds was not significantly different (P > 0.05) from *fab1-1 fae1 fad2* (Fig. 4C).

299　AGPAT1 expression therefore allows a higher incorporation of 16:0 into the sn-2 position of TG

300　in WT and HPHO seeds than mLPAT1 (van Erp et al., 2019).
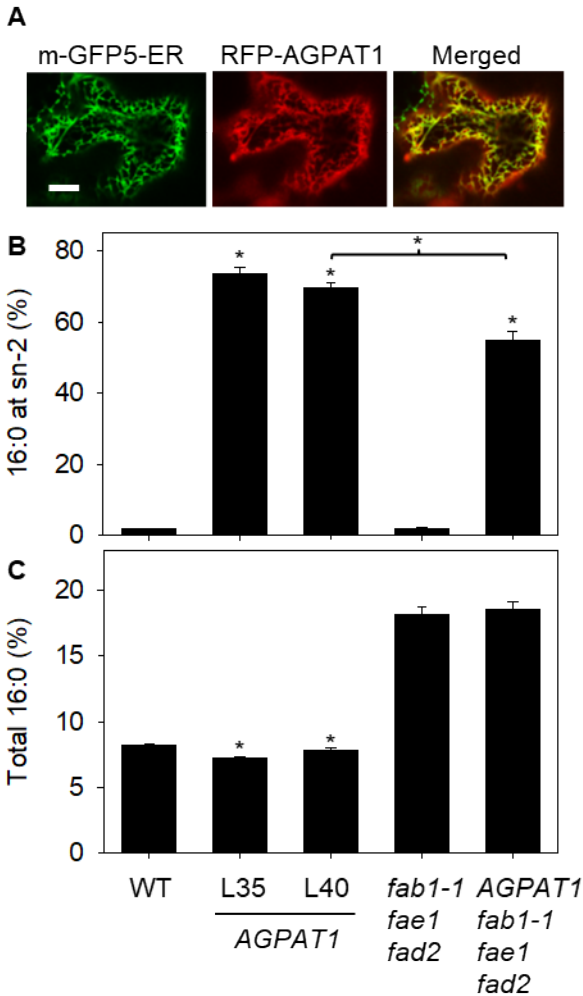
Fig. 4. 16:0 in TG from WT and HPHO seeds expressing *AGPAT1*. Laser scanning confocal microscopy image of a *N. benthamiana* epidermal cell transiently expressing RFP-AGPAT1 and m-GFP5-ER marker (A). Scale bar = 20 μm. Percentage of 16:0 esterified to the sn-2 position (B) and 16:0 as a percentage of total FA content (C) measured in TG isolated from WT, *ProGLY:AGPAT1*, *fab1-1 fad2 fae1* and *ProGLY:AGPAT1 fab1-1 fad2 fae1* seeds. Values are the mean ± SE of measurements on seeds from three plants of each genotype. * denote values significantly (P < 0.05) different either from WT or *fab1-1 fad2 fae1*, and where marked in parenthesis, from one another (ANOVA + Tukey HSD test).

3.4. Disruption of LPAT2 and PDCT enhances mLPAT1 and AGPAT1-dependent 16:0 incorporation into the sn-2 position of TG in HPHO seeds

313　In wild type (WT) Arabidopsis seeds we previously found that mLPAT1-dependent
314　incorporation of 16:0 into the sn-2 position of TG could be increased by disrupting the enzymes
315　LPAT2 and PDCT (van Erp et al., 2019). *LPAT2* is an essential gene in Arabidopsis and encodes
316　the main ER-localized LPAT isoform in seeds (Kim et al., 2005). Disruption of *LPAT2,* using the
317　hypomorphic *lpat2-3* allele, reduces competition with mLPAT1 (Fig. 1) (van Erp et al., 2015).
318　PDCT catalyses DG-PC interconversion in Arabidopsis seeds and its disruption, using the *pdct*
319　mutant (Lu et al., 2009), forces a more direct flux of newly made DG into TG, helping to bypass
320　acyl-editing at the sn-2 position in PC (Fig. 1) (Bates et al., 2012). To determine whether LPAT2
321　and PDCT disruption affect the percentage of 16:0 esterified to the sn-2 position in TG in HPHO
322　seeds expressing mLPAT1 or AGPAT1, we constructed *ProGLY:mLPAT1 fab1-1 fae1 fad2*
323　*lpat2-3 pdct* and *ProGLY:AGPAT1 fab1-1 fae1 fad2 lpat2-3 pdct* lines by crossing. When we
324　purified TG from these seeds and performed positional analysis, we found that the percentage of
325　16:0 at the sn-2 position, was about 62% and 84%, respectively (Fig. 5A). The total 16:0 content
326　in *ProGLY:mLPAT1 fab1-1 fae1 fad2 lpat2-3 pdct* and *ProGLY:AGPAT1 fab1-1 fae1 fad2 lpat2-*
327　*3 pdct* seeds was around 25 and 23%, respectively (Fig. 5B). The levels of 16:0 enrichment at sn-
328　2 therefore compare favourably to that of human milk fat (Giuffrida et al., 2018) and the TG
329　molecular species composition is also dominated by the combined regioisomers and enantiomers
330　of OPO (Table 1). Indeed, it is possible to estimate that OPO likely accounts for more than 30%
331　of all TG molecular species in *ProGLY:mLPAT1 fab1-1 fae1 fad2 lpat2-3 pdct* seeds and more
332　than 40% in *ProGLY:AGPAT1 fab1-1 fae1 fad2 lpat2-3 pdct* seeds, given the percentages of
333　16:0 at *sn-2* (Fig. 5A) and abundances of OPO regioisomers and enantiomers (Table 1).
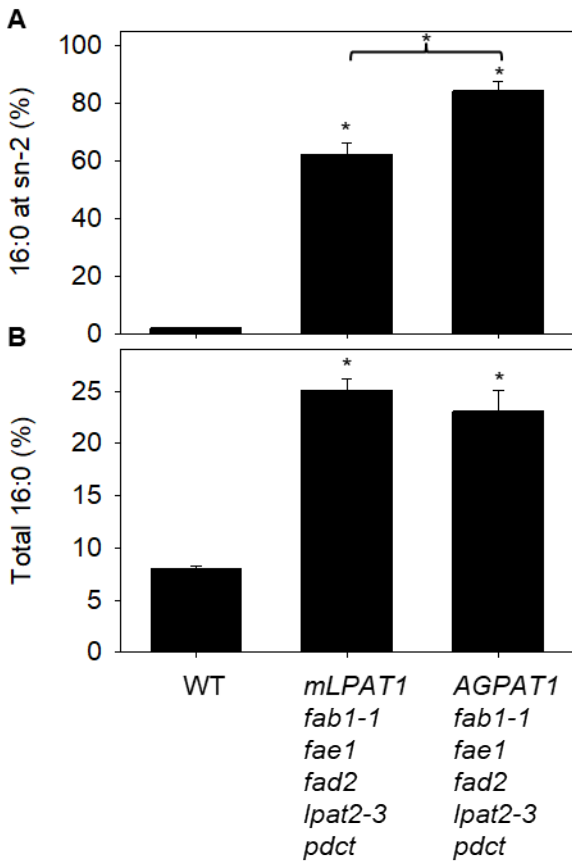
Fig. 5. 16:0 in TG from HPHO *lpat2-3 pdct* seeds expressing *mLPAT1* or *AGPAT1*. Percentage of 16:0 esterified to the sn-2 position (A) and 16:0 as a percentage of total FA content (B) measured in TG isolated from WT, *ProGLY:mLPAT1 fab1-1 fae1 fad2 lpat2-3 pdct* and *ProGLY:AGPAT1 fab1-1 fae1 fad2 lpat2-3 pdct* seeds. Values are the mean ± SE of measurements on seeds from three plants of each genotype. * denote values significantly ($P < 0.05$) different either from WT or, where marked in parenthesis, from one another (ANOVA + Tukey HSD test).

Table 1. TG composition of HPHO *lpat2-3 pdct* seeds expressing *mLPAT1* or *AGPAT1*.

TG species	Genotype	
	ProGLY:mLPAT1 fab1-1 fae1 fad2 lpat2-3 pdct	*ProGLY:AGPAT1 fab1-1 fae1 fad2 lpat2-3 pdct*
50:2 (16:0_16:1_18:1)	0.95 ±0.07	0.32 ±0.02
52:2 (16:0_18:1_18:1)	53.93 ±1.37	50.14 ±0.11
52:3 (16:1_18:1_18:1)	2.11 ±0.15	0.77 ±0.02
52:4 (16:0_18:1_18:3)	0.89 ±0.05	0.37 ±0.02
54:2 (18:0_18:1_18:1)	2.70 ±0.28	3.97 ±0.16
54:3 (18:1_18:1_18:1)	29.47 ±0.27	34.36 ±0.40
54:4 (18:1_18:1_18:2)	1.21 ±0.05	1.63 ±0.03
54:5 (18:1_18:1_18:3)	2.21 ±0.13	2.21 ±0.07
56:2 (20:0_18:1_18:1)	0.95 ±0.10	1.19 ±0.04
56:3 (20:1_18:1_18:1)	1.17 ±0.46	1.52 ±0.41

Values are expressed as a percentage of total and are the mean ± SE of measurements on seeds from four plants of each genotype. Only TG species that account for >1% of the total in at least one genotype are shown.

3.5. HPHO seeds have a modest reduction in oil content and seed vigour but this is not compounded by redistribution of 16:0 to the sn-2 position

Modification of FA composition can reduce TG accumulation in oilseeds and can also impair seed germination and seedling establishment (Lunn et al., 2017; Bai et al., 2019). We previously found that *ProGLY:mLPAT1 lpat2-3 pdct* seeds, which have a low total 16:0 content but about 70% esterified to the sn-2 position, exhibit a reduction in TG content as a percentage of seed weight (van Erp et al., 2019). However, their germination and initial seedling growth were not significantly impaired (van Erp et al., 2019). To examine the physiological impact of 16:0 enrichment at the sn-2 position of TG in HPHO seeds, we compared seed batches from WT, *fab1-1 fae1 fad2, ProGLY:mLPAT1 fab1-1 fae1 fad2 lpat2-3 pdct* and *ProGLY:AGPAT1 fab1-1 fae1 fad2 lpat2-3 pdct* plants that had been grown together under standard laboratory conditions. We found that both seed weight and percentage oil content were significantly reduced (P > 0.05)

361 in *fab1-1 fae1 fad2* relative to WT (Fig. 6). However, no significant difference was observed

362 between *fab1-1 fae1 fad2* and *ProGLY:mLPAT1 fab1-1 fae1 fad2 lpat2-3 pdct* or

363 *ProGLY:AGPAT1 fab1-1 fae1 fad2 lpat2-3 pdct* seeds (Fig. 6). These data suggest that TG

364 biosynthetic flux is impaired in *fab1-1 fae1 fad2* seeds, but that the further genetic modifications

365 leading to incorporation of 16:0 into the sn-2 position of TG are not detrimental in this

366 background. These findings contrast with what we observed in WT seeds (van Erp et al., 2019).
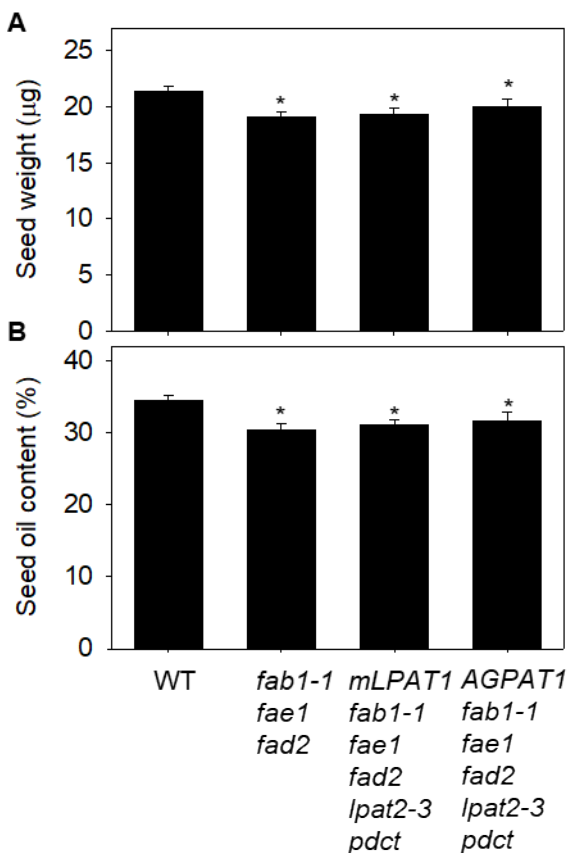
Fig. 6. Oil content of HPHO *lpat2-3 pdct* seeds expressing *mLPAT1* or *AGPAT1*. Seed weight
(A) and percentage oil content (B) of WT, *fab1-1 fae1 fad2, ProGLY:mLPAT1 fab1-1 fae1 fad2 lpat2-3 pdct* and *ProGLY:AGPAT1 fab1-1 fae1 fad2 lpat2-3 pdct* seeds. Values are the mean ±
SE of measurements on seeds from five plants of each genotype. * denote values significantly ($P < 0.05$) different either from WT (ANOVA + Tukey HSD test).

In standard laboratory conditions (20°C, 16h photoperiod), the speed of *fab1-1 fae1 fad2* seed germination (scored as radicle emergence) and seedling establishment (scored as cotyledon expansion) was significantly slower ($P > 0.05$) than WT (Fig. 7). However, no significant difference ($P > 0.05$) was observed between *fab1-1 fae1 fad2* and *ProGLY:mLPAT1 fab1-1 fae1 fad2 lpat2-3 pdct* or *ProGLY:AGPAT1 fab1-1 fae1 fad2 lpat2-3 pdct* seeds (Fig. 7). These data suggest that seed vigour is impaired in *fab1-1 fae1 fad2* seeds, but that incorporation of 16:0 into the sn-2 position of TG does not compound this phenotype.
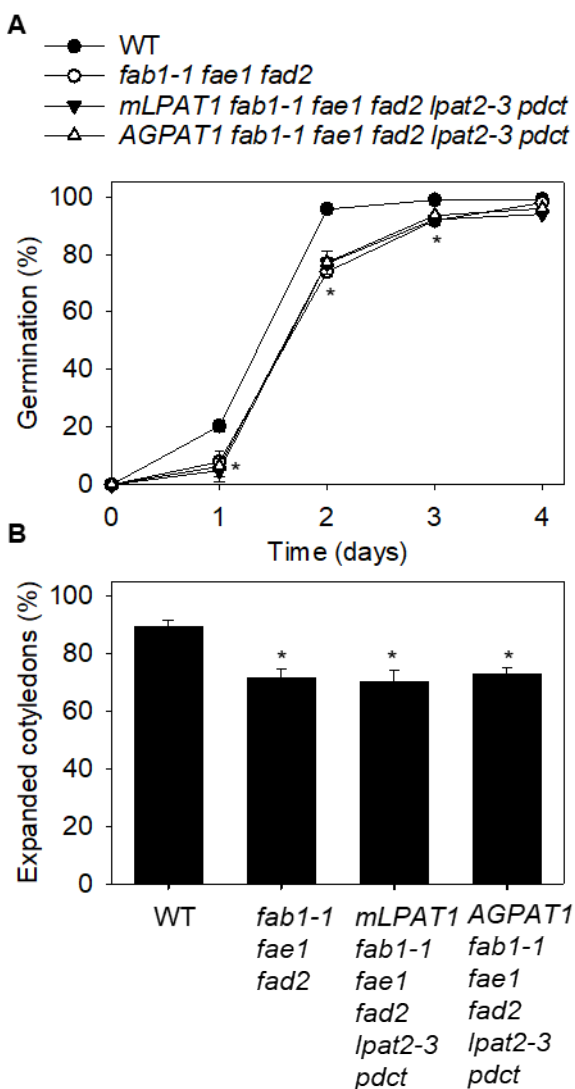
Fig. 7. Vigour of HPHO *lpat2-3 pdct* seeds expressing *mLPAT1* or *AGPAT1*. Percentage seed germination (A) and cotyledons fully expanded by day 4 (B) of WT, *fab1-1 fae1 fad2*, *ProGLY:mLPAT1 fab1-1 fae1 fad2 lpat2-3 pdct* and *ProGLY:AGPAT1 fab1-1 fae1 fad2 lpat2-3*

18

386 *pdct* seeds. Values are the mean ± SE of measurements on seeds from three plants of each
387 genotype. * denote values significantly (P < 0.05) different either from WT (ANOVA + Tukey
388 HSD test).

389

390 **4. Discussion**

391

392 In this study we show that Arabidopsis seeds can be engineered to produce OPO, since their TG
393 contains around 20% 16:0 and 70% 18:1, with more than 80% of the 16:0 esterified to the sn-2
394 position on the glycerol backbone. The combined regioisomers and enantiomers of OPO account
395 for around 50% of the TG species and OPO therefore likely constitutes around 40%. OPO is
396 commonly the main TG molecular species present in human milk (Giuffrida et al., 2018), but it
397 is virtually absent from vegetable oils, which typically contain very little 16:0 esterified to the
398 sn-2 position (Brockerhoff and Yurkowsk, 1966; Christie et al., 1991). The high OPO content of
399 human milk is believed to confer nutritional benefits (Innis 2011; Béghin et al., 2018) and
400 therefore the development of a vegetable oil that is rich in OPO might provide a new source of
401 ingredient for infant formulas (van Erp et al., 2019). Microbial oils are also used for human
402 nutrition and it is noteworthy that oleaginous yeasts grown on glucose also exclude 16:0 for the
403 sn-2 position of their TG (Thorpe and Ratledge, 1972).

404 We previously showed that lipid metabolism in Arabidopsis seeds can be engineered so
405 that about 70% of the 16:0 present in the TG can occupy the sn-2 position (van Erp et al., 2019).
406 However, wild type Arabidopsis seeds do not have the appropriate FA composition necessary to
407 mimic that of human milk, which is much richer in both 16:0 and 18:1 (Wei et al., 2019). We
408 therefore produced an Arabidopsis HPHO multi-mutant background with about 20% 16:0 and
409 70% 18:1 by combining *fab1-1* (Wu et al., 1994), *fae1* (James et al., 1995) and *fad2* (Miquel and
410 Browse, 1992) alleles. Fernández-Martínez et al., (1997) also developed a conventional HPHO
411 sunflower (*Helianthus annuus*) variety with seeds containing about 30% 16:0 and 55% 18:1 by
412 combining *fab1* and *fad2* mutant alleles (Perez-Vich et al., 2016; Schuppert et al., 2006).

413 The expression of an ER-retargeted version of the chloroplast LPAT (mLPAT1) in WT
414 Arabidopsis seeds allows 30 to 40% of the 16:0 present in the TG to occupy the sn-2 position
415 (van Erp et al., 2019). However, when we expressed mLPAT1 in the HPHO background, we
416 found the incorporation of 16:0 into the sn-2 position was reduced to about 20%. Disruption of

417   LPAT2 and PDCT then lead to an increase in the percentage of 16:0 at sn-2 to about 62%. This

418   level of 16:0 enrichment at sn-2 is also lower than we were able to achieve in WT using the same

419   approach (van Erp et al., 2019). However, the total FA composition of HPHO is more

420   appropriate for an infant formula ingredient and 62% 16:0 at sn-2 still compares quite favourably

421   with commercially available HMFS that are produced using 1,3-regiospecific lipases (Wei et al.,

422   2019).

423   Generally, in human milk fat more than 70% of the 16:0 is esterified to the sn-2 position

424   of TG and this level of enrichment therefore remains the target for HMFS. The human LPAT

425   AGPAT1 can use 16:0-CoA as a substrate (Agarwal et al., 2011) and appears to be expressed in

426   lactocytes (Lamay et al., 2013). When we expressed AGPAT1 in WT Arabidopsis seeds we

427   found that 60 to 70% of the 16:0 present in the TG occupied the sn-2 position. This level of

428   enrichment is approximately twice as high as we previously achieved through expression of

429   mLPAT1 (van Erp et al., 2019). LPAT1 is a chloroplast enzyme that uses a 16:0-ACP substrate

430   *in vivo* (Bourgis et al., 1999), it is therefore likely to be less well adapted than AGPAT1 to

431   function in the ER and use an acyl-CoA substrate (Agarwal et al., 2011). When we expressed

432   AGPAT1 in a HPHO background, incorporation of 16:0 into the sn-2 position was reduced to

433   about 54%, but disruption of LPAT2 and PDCT then lead to an increase in the percentage of

434   16:0 at sn-2 to about 84%. This level of enrichment of 16:0 at sn-2 is greater than or equal to that

435   reported in human milk fat (Giuffrida et al., 2018).

436   Collectively, our data suggest that when the relative amount of 16:0 (and 18:1) are

437   increased in Arabidopsis seeds, mLPAT1 and AGPAT1 incorporate a lower percentage of 16:0

438   into the sn-2 position of TG. Although LPAT activity is of primary importance in determining

439   what type of acyl group is esterified to the sn-2 position, the acyl distribution across positions is

440   also influenced by the activities of the acyltransferases responsible for esterifying the sn-1 and

441   sn-3 positions, and by the availability of their substrates. In Arabidopsis, GLYCEROL-3-

442   PHOSPHATE ACYLTRANSFERASE 9 (GPAT9) (Shockey et al., 2016; Singer et al., 2016)

443   and DIACYLGLYCEROL ACYLTRANSFERASE 1 (DGAT1) (Hobbs et al., 1999; Routaboul

444   et al., 1999; Zou et al., 1999) are likely to be responsible for esterifying most of the acyl groups

445   to the sn-1 and sn-3 position, respectively. These enzymes may compete with native and/or

446   heterologous LPATs for acyl-CoA substrates. To achieve a substantially higher enrichment of

447   16:0 at sn-2 than 84% in Arabidopsis HPHO seeds it may be necessary to exclude 16:0 from the

448   sn-1 and sn-3 positions by replacing GPAT9 and DGAT1 with isoforms that exhibit a stronger
449   selectivity for unsaturated acyl-CoAs.

450   Metabolic pathway engineering can often have detrimental effects on TG accumulation in
451   oilseeds and can also impair seed vigour (Lunn et al., 2017; Bai et al., 2019). We previously
452   found that redirecting 16:0 to the sn-2 position of TG in WT Arabidopsis seeds reduced oil
453   accumulation (van Erp et al., 2019). HPHO seeds also have a slightly lower seed oil content than
454   WT. However, engineering a similar shift in positional distribution of 16:0 did not lead to a
455   further reduction. Given that WT seeds have a about 3-fold lower 16:0 content than HPHO
456   seeds, it may be that low 16:0 availability restricts the rate of TG biosynthesis in seeds
457   engineered to possess mainly 16:0-CoA LPAT activity in their ER. Conversely, the
458   approximately 3-fold higher 16:0 content in HPHO seeds might conceivably restrict TG
459   biosynthesis because the native LPATs (and other acyltransferase activities) have too little 16:0-
460   CoA activity. HPHO seeds are also significantly impaired in the speed of seed germination and
461   early seedling growth, although they do establish. Redirecting 16:0 to the sn-2 position of TG in
462   HPHO seeds does not appear to compound this phenotype. Poorer HPHO seed vigour may be
463   caused by the reduction in long-chain FA unsaturation, which raises the melting temperature of
464   the oil (Sun et al., 2014). This property is not so greatly influenced by the positional distribution
465   of the FA.

466   HPHO plants are also impaired in vegetative growth, exhibiting slightly smaller rosettes
467   and shorter stems at maturity. FAB1 and FAD2 play constitutive roles in Arabidopsis lipid
468   metabolism and the vegetative phenotypes in HPHO likely result from the combined
469   perturbations in membrane lipid composition (Wu et al., 1994; Miquel and Browse, 1992).
470   Under stresses, such as low temperature, these phenotypes may also become more pronounced
471   (Wu et al., 1997; Miquel and Browse, 1994). Adverse effects can be avoided in vegetative
472   tissues of oilseed crops by using seed-specific promoters to drive *FAB1* and *FAD2* RNA
473   interference (Nguyen et al., 2013; 2015). Crops like canola (*Brassica napus*) and false flax
474   (*Camelina sativa*) are amenable to genetic engineering and are therefore potential platforms for
475   OPO production, using the transgenic approach we describe here. Transgene expression in plants
476   can be lost over generations owing to gene silencing, but both the *ProGLY:mLPAT1* and
477   *ProGLY:AGPAT1* lines used in this study appear to be quite stable, having maintained their
478   phenotypes for six generations (Supplementary Table 2).

479

Authorship contributions

P.J.E. conceived the research plans and supervised the experiments; H.vE., L.V.M. and P.J.E. performed the experiments; F.M.B. and J.M-M. provided technical assistance to H.vE.; P.J.E., H.vE. and L.V.M. designed the experiments and analysed the data; P.J.E. conceived the project and wrote the article with contributions of all the authors.

Conflicts of interest

The authors declare there is no conflict of interest.

References

Agarwal AK, Sukumaran S, Cortés VA, Tunison K, Mizrachi D, Sankella S, Gerard RD, Horton JD, Garg A (2011) Human 1-acylglycerol-3-phosphate O-acyltransferase isoforms 1 and 2: biochemical characterization and inability to rescue hepatic steatosis in Agpat2(-/-) gene lipodystrophic mice. J Biol Chem 286: 37676-37691

504

505   Bai S, Engelen S, Denolf P, Wallis JG, Lynch K, Bengtsson JD, Thournout MV, Haesendonckx
506   B, Browse J (2019) Identification, characterization and field testing of Brassica napus mutants
507   producing high-oleic oils. Plant J 98: 33-41

509   Bates PD, Fatihi A, Snapp AR, Carlsson AS, Browse J, Lu C (2012) Acyl editing and headgroup
510   exchange are the major mechanisms that direct polyunsaturated fatty acid flux into
511   triacylglycerols. Plant Physiol 160: 1530-1539

513   Bates PD, Browse J (2011) The pathway of triacylglycerol synthesis through
514   phosphatidylcholine in Arabidopsis produces a bottleneck for the accumulation of unusual fatty
515   acids in transgenic seeds. Plant J 68: 387-399.

517   Béghin L, Marchandise X, Liend E, Bricoute M, Bernete J-P, Lienhardte J-F, Jeannerote F,
518   Menete V, Requillarte J-C, Marx J, et al. (2018) Growth, stool consistency and bone mineral
519   content in healthy term infants fed sn-2-palmitate-enriched starter infant formula: A randomized,
520   double-blind, multicentre clinical trial. Clin Nutr 38: 1023-1030

522   Bourgis F, Kader J-C, Barret P, Renard M, Robinson D, Robinson C, Delseny M, Roscoe TJ
523   (1999) A plastidial lysophosphatidic acid acyltransferase from oilseed rape. Plant Physiol 120:
524   913-922

526   Breckenridge WC, Marai L, Kuksis A (1969) Triglyceride structure of human milk fat. Can J
527   Biochem 47: 761-769

529   Brockerhoff H, Yurkowsk M (1966) Stereospecific analyses of several vegetable fats. J Lipid
530   Res 7: 62-64

532 Carlsson AS, LaBrie ST, Kinney AJ, von Wettstein-Knowles P, Browse J (2002) A KAS2 cDNA

533 complements the phenotypes of the Arabidopsis fab1 mutant that differs in a single residue

534 bordering the substrate binding pocket. Plant J 29: 761-70

535

536 Christie WW, Nikolova-Damyanova B, Laakso P, Herslof B (1991) Stereospecific analysis of

537 triacyl-sn-glycerols via resolution of diastereomeric diacylglycerol derivatives by high-

538 performance liquid chromatography on silica. J Am Oil Chem Soc 68: 695-701

539

540 Clough SJ, Bent AF (1998) Floral dip: a simplified method for Agrobacterium-mediated

541 transformation of Arabidopsis thaliana. Plant J 16: 735–43

542

543 Fernández-Martínez JM, Mancha M, Osorio J, Garcés R (1997) Sunflower mutant containing

544 high levels of palmitic acid in high oleic background. Euphytica 97: 113-116

545

546 Ferreira-Dias S, Tecelão C (2014) Human milk fat substitutes: Advances and constraints of

547 enzyme□catalyzed production. Lipid technology 26: 183-186

548

549 Frentzen M, Heinz E, McKeon TA, Stumpf PK (1983) Specificities and selectivities of glycerol-

550 3-phosphate acyltransferase and monoacylglycerol-3-phosphate acyltransferase from pea and

551 spinach chloroplasts. Eur J Biochem 129: 629-636

552

553 Giuffrida F, Marmet C, Tavazzi I, Fontannaz P, Sauser J, Lee LY, Destaillats F (2018)

554 Quantification of 1,3-olein-2-palmitin (OPO) and Palmitic Acid in sn-2 Position of

555 Triacylglycerols in Human Milk by Liquid Chromatography Coupled with Mass Spectrometry.

556 Molecules 24: pii: E22

557

558 Hobbs DH, Lu C, Hills MJ (1999) Cloning of a cDNA encoding diacylglycerol acyltransferase

559 from Arabidopsis thaliana and its functional expression. FEBS Lett 452: 145–149

560

561 Innis SM (2011) Dietary triacylglycerol structure and its role in infant nutrition. Adv Nutr 2:
562 275-283

563

564 James DW Jr, Dooner HK (1991) Novel seed lipid phenotypes in combinations of mutants
565 altered in fatty acid biosynthesis in Arabidopsis. Theor Appl Genet 82: 409-412

566

567 James DW Jr, Lim E, Keller J, Plooy I, Ralston E, Dooner HK (1995) Directed tagging of the
568 Arabidopsis FATTY ACID ELONGATION1 (FAE1) gene with the maize transposon activator.
569 Plant Cell 7: 309-319

570

571 Joyard J, Douce R (1977) Site of synthesis of phosphatidic acid and diacyglycerol in spinach
572 chloroplasts. Biochim Biophys Acta 486: 273-285

573

574 Kim HU, Li Y, Huang AH (2005) Ubiquitous and endoplasmic reticulum-located
575 lysophosphatidyl acyltransferase, LPAT2, is essential for female but not male gametophyte
576 development in Arabidopsis. Plant Cell 17: 1073-1089

577

578 Kelly AA, van Erp H, Quettier A-L, Shaw E, Menard G, Kurup S, Eastmond PJ (2013) The
579 SUGAR-DEPENDENT1 lipase limits triacylglycerol accumulation in vegetative tissues of
580 Arabidopsis. Plant Physiol 162: 1282-1289

581

582 Lemay DG, Ballard OA, Hughes MA, Morrow AL, Horseman ND, Nommsen-Rivers LA (2013)
583 RNA sequencing of the human milk fat layer transcriptome reveals distinct gene expression
584 profiles at three stages of lactation. PLoS One 8: e67531

585

586 Lu C, Xin Z, Ren Z, Miquel M, Browse J (2009) An enzyme regulating triacylglycerol
587 composition is encoded by the ROD1 gene of Arabidopsis. Proc Natl Acad Sci USA 106: 18837-
588 18842

589

590   Lunn D, Smith GA, Wallis JG, Browse J (2018) Development defects of hydroxy-fatty acid-
591   accumulating seeds are reduced by castor acyltransferases. Plant Physiol 177: 553-564

592

593   Millar AA, Kunst L (1997) Very-long-chain fatty acid biosynthesis is controlled through the
594   expression and specificity of the condensing enzyme. Plant J 12: 121-131

595

596   Miquel M, Browse J (1992) Arabidopsis mutants deficient in polyunsaturated fatty acid
597   synthesis. Biochemical and genetic characterization of a plant oleoyl-phosphatidylcholine
598   desaturase. J Biol Chem 267: 1502-1509

599

600   Miquel MF, Browse JA (1994) High-oleate oilseeds fail to develop at low temperature. Plant
601   Physiol 106: 421–427

602

603   Nguyen HT, Silva JE, Podicheti R, Macrander J, Yang W, Nazarenus TJ, Nam J-W, Jaworski
604   JG, Lu C, Scheffler BE, Mockaitis K, Cahoon EB (2013) Camelina seed transcriptome: a tool for
605   meal and oil improvement and translational research. Plant Biotechnol J 11: 759-769

606

607   Nguyen HT, Park H, Koster KL, Cahoon RE, Nguyen HT, Shanklin J, Clemente TE, Cahoon EB
608   (2015) Redirection of metabolic flux for high levels of omega-7 monounsaturated fatty acid
609   accumulation in camelina seeds. Plant Biotechnol J 13: 38-50

610

611   Ohlrogge J, Browse J (1995) Lipid Biosynthesis. Plant Cell 7: 957-970

612

613   Okuley J, Lightner J, Feldmann K, Yadav N, Lark E, Browse J (1994) Arabidopsis FAD2 gene
614   encodes the enzyme that is essential for polyunsaturated lipid synthesis. Plant Cell 6: 147-158

615

616   Perez-Vich B, del Moral L, Velasco L, Bushman BS, Knapp SJ, Leon A, Fernández-Martínez
617   JM, Berry ST (2016) Molecular basis of the high-palmitic acid trait in sunflower seed oil. Mol
618   Breed 36: 43

619

620   Pidkowich MS, Nguyen HT, Heilmann I, Ischebeck T, Shanklin J (2007) Modulating seed beta-

621   ketoacyl-acyl carrier protein synthase II level converts the composition of a temperate seed oil to

622   that of a palm-like tropical oil. Proc Natl Acad Sci USA 104: 4742-4747

623

624   Routaboul JM, Benning C, Bechtold N, Caboche M, Lepiniec L (1999) The TAG1 locus of

625   Arabidopsis encodes for a diacylglycerol acyltransferase. Plant Physiol Biochem 37: 831–840

626

627   Schuppert GF, Tang S, Slabaugh MB, Knapp SJ (2006) The sunflower high-oleic mutant Ol

628   carries variable tandem repeats of FAD2-1, a seed-specific oleoyl-phosphatidyl choline

629   desaturase. Mol Breed 17: 241–256

630

631   Shockey J, Regmi A, Cotton K, Adhikari N, Browse J, Bates PD (2016) Identification of

632   Arabidopsis GPAT9 (At5g60620) as an essential gene involved in triacylglycerol biosynthesis.

633   Plant Physiol 170: 163–179

634

635   Singer SD, Chen G, Mietkiewska E, Tomasi P, Jayawardhane K, Dyer JM, Weselake RJ (2016)

636   Arabidopsis GPAT9 contributes to synthesis of intracellular glycerolipids but not surface lipids.

637   J Exp Bot 67: 4627–4638

638

639   Smith MA, Moon H, Chowrira G, Kunst L (2003) Heterologous expression of a fatty acid

640   hydroxylase gene in developing seeds of Arabidopsis thaliana. Planta 217: 507–516

641

642   Stymne S, Stobart AK (1984) Evidence for the reversibility of the acyl-

643   CoA:lysophosphatidylcholine acyltransferase in microsomal preparations from developing

644   safflower (Carthamus tinctorius L.) cotyledons and rat liver. Biochem J 223: 305-314

645

646   Sun J-Y, Hammerlindl J, Forseille L, Zhang H, Smith MA (2014) Simultaneous over-expressing

647   of an acyl-ACP thioesterase (FatB) and silencing of acyl-acyl carrier protein desaturase by

648 artificial microRNAs increases saturated fatty acid levels in Brassica napus seeds. Plant Biotech
649 J 12: 624–637

650

651 Thorpe RF and Ratledge C (1972) Fatty acid distribution in triglycerides of yeasts grown on
652 glucose or n-alkanes. Microbiology 72, 151.

653

654 van Erp H, Bates PD, Burgal J, Shockey J, Browse J (2011) Castor phospholipid:diacylglycerol
655 acyltransferase facilitates efficient metabolism of hydroxy fatty acids in transgenic Arabidopsis.
656 Plant Physiol 155: 683-693

657

658 van Erp H, Bryant FM, Martin-Moreno J, Michaelson LV, Bhutada G, Eastmond PJ (2019)
659 Engineering the stereoisomeric structure of seed oil to mimic human milk fat. Proc Natl Acad Sci
660 USA 116: 20947–20952

661

662 van Erp H, Kelly AA, Menard G, Eastmond PJ (2014) Multigene engineering of triacylglycerol
663 metabolism boosts seed oil content in Arabidopsis. Plant Physiol 165: 30-36

664

665 van Erp H, Shockey J, Zhang M, Adhikari ND, Browse J (2015) Reducing isozyme competition
666 increases target fatty acid accumulation in seed triacylglycerols of transgenic Arabidopsis. Plant
667 Physiol 168: 36-46

668

669 Wang L, Shen W, Kazachkov M, Chen G, Chen Q, Carlsson AS, Stymne S, Weselake RJ, Zou J
670 (2012) Metabolic interactions between the Lands cycle and the Kennedy pathway of glycerolipid
671 synthesis in Arabidopsis developing seeds. Plant Cell 24: 4652-4669

672

673 Wei W, Jin Q, Wang X (2019) Human milk fat substitutes: Past achievements and current trends.
674 Prog Lipid Res 74: 69-86

675

676   West AL, Michaelson LV, Miles EA, Haslam RP, Lillycrop KA, Georgescu R, Han L, Napier

677   JA, Calder PC, Burdge GC (2020) Lipidomic analysis of plasma from healthy men and women

678   shows phospholipid class and molecular species differences between sexes. Lipids doi:

679   10.1002/lipd.12293.

680

681   Witkowska-Zimny M, Kaminska-El-Hassan E (2017) Cells of human breast milk. Cell Mol Biol

682   Lett 22: 11

683

684   Wood CC, Petrie JR, Shrestha P, Mansour MP, Nichols PD, Green AG, Singh SP (2009) A leaf-

685   based assay using interchangeable design principles to rapidly assemble multistep recombinant

686   pathways. Plant Biotech J 7: 914-924

687

688   Wu J, James DW Jr, Dooner HK, Browse J (1994) A mutant of Arabidopsis deficient in the

689   elongation of palmitic acid. Plant Physiol 106: 143-150

690

691   Wu J, Lightner J, Warwick N, Browse J (1997) Low-temperature damage and subsequent

692   recovery of *fab1* mutant Arabidopsis exposed to 2°C. Plant Physiol 113: 347–356

693

694   Zhang C, Cahoon RE, Hunter SC, Chen M, Han J, Cahoon EB (2013) Genetic and biochemical

695   basis for alternative routes of tocotrienol biosynthesis for enhanced vitamin E antioxidant

696   production. Plant J. 73: 628–639

697

698   Zou JT, Wei YD, Jako C, Kumar A, Selvaraj G, Taylor DC (1999) The Arabidopsis thaliana

699   TAG1 mutant has a mutation in a diacylglycerol acyltransferase gene. Plant J 19: 645–653